Optimizing enhanced coalbed methane recovery for unhindered production and CO_2 injectivity

Hemant Kumar [a,*], Derek Elsworth [a], Jishan Liu [b], Denis Pone [c], Jonathan P. Mathews [a]

[a] John and Willie Leone Department of Energy and Mineral Engineering, EMS Energy Institute and G^3 Center, Pennsylvania State University, University Park, PA 16802, USA
[b] School of Mechanical Engineering, University of Western Australia, WA 6009, Australia
[c] ConocoPhillips, Bartlesville, OK, USA

ARTICLE INFO

ABSTRACT

We explore the effect of gas pressure and stress on the permeability evolution of coalbed methane (CBM) reservoirs infiltrated by carbon dioxide (CO_2). Typically the recovery of methane induces shrinkage and the injection of CO_2 induces swelling respectively increasing or decreasing permeability for constrained coals. Permeability evolution was quantified for moisture equilibrated and partially dried bituminous coal samples together with the transitions caused by sequential exposure to different gases. We report experimental measurements of permeability evolution in a coal from the Uinta basin infiltrated by helium (He), methane (CH_4) and CO_2 under varying gas pressure (1–8 MPa) and moisture content (1–9% by mass) while subjected to constant applied stresses (10 MPa). Permeability decreases with increased moisture content for all the gases (He, CH_4 and CO_2). The decrease in He permeability may be as high as ∼100 fold if the moisture content is increased from 1 to 9%. Swelling induced by sorption of CH_4 and CO_2 in the coal matrix reduces permeability by 5–10 fold depending on the gas injected and the moisture content. Swelling increases with gas pressure to a maximum (strain based estimation 5%) at a critical pressure (∼4.1 MPa) corresponding to maximum adsorption capacity. Beyond this threshold effective stress effects dominate. We use permeability evolution in bituminous coal for various moisture contents, effective stresses, and gas pressures to propose a mechanistic model. Also, we showcase this model to explain the published data for permeability evolution on water saturated Pennsylvanian anthracite coal. We use this model to investigate the performance of prototypical ECBM projects. In particular we examine the effect of the permeability loss with injection of CO_2. We define response in terms of two conditions: reservoirs either below (under) or above (over) the saturation pressure that defines the permeability minima in the reservoir. For oversaturated reservoirs withdrawal will always result in decreased permeability at the withdrawal well unless the critical pressure is transited. Similarly permeability will decrease at the CO_2 injection well unless the pressure increase is sufficiently large to overcome the reduction in permeability due to CO_2 – typically of order of one to a few MPa. For undersaturated reservoirs the permeability will always increase at the withdrawal well and can only increase at the injection well if the critical pressure is transited and further exceeded by one to a few MPa. These observations provide a rational method to design injection and recovery strategies for ECBM that account for the complex behavior of the reservoir including the important effects of moisture content, gas composition and effective stress.

© 2012 Elsevier Ltd. All rights reserved.

1. Introduction

Full scale exploration in the Uinta basin began in the 1990s. This basin has 10 trillion cubic feet of recoverable CBM reserves (EPA, 2004). There were 500 CBM wells in the basin with cumulative production of 75.7 billion cubic feet in 2000 (EPA, 2004). The Uinta basin has high CH_4 content ranging from 250 to 400 scf/ton (US-DOE, 2004) with the highest recovery factor amongst all the basins at 89% (Reeves, 2003). Injection of CO_2 in unmineable coal seams provides 'value-added' sequestration with benefits such as enhanced coalbed methane recovery with lower net-cost (Reeves, 2003), making unmineable coals potentially attractive sequestration sites. Coalbeds are commonly self-sourcing and low permeability (on the order of fractions of milliDarcies) gas reservoirs with recovery enabled through reservoir pressure depletion by water removal (Rogers, 1994). Various studies on laboratory and pilot plant scales demonstrate that geomechanical processes coupled with gas uptake or loss evolution during the ECBM recovery process affect the dynamic permeability and hence production (Gu and Chalaturnyk, 2005; van Bergen et al., 2009).

Coal shrinkage and swelling with gas desorption/adsorption has an important influence on the evolution of permeability (Bustin et al., 2008; Cui et al., 2007; Harpalani and Chen, 1995; Kelemen et al., 2006; Seidle and Huitt, 1995). Coal swells with adsorption of CO_2 and develops compactive stresses if mechanically constrained (Day et al., 2010; Pone et al., 2010; Reucroft and Patel, 1986; Siemons and Busch, 2007). Coal swelling has been implicated as observed reductions in permeabilities during ECBM operations at pilot plant scale (Durucan and Shi, 2009; Kiyama et al., 2011; van Bergen et al., 2006). Gas adsorption and related swelling is largely impacted by sorption capacity, coal rank and the composition of the permeating gas (Chikatamarla et al., 2004a, b; Levine, 1996; Pone et al., 2010). The uptake of gas by coal at various pore pressures is often represented by the sorption isotherm (Kelemen et al., 2006; Levine, 1996). The preferential sorption of CO_2 over CH_4 results in net swelling of the coal matrix (Chikatamarla et al., 2004b; Gu and Chalaturnyk, 2005; Levine, 1996) that closes or reduces the aperture of existing cleats and result in a net reduction in permeability during CO_2 injection for constrained coals. At higher gas pressures, this reduction in permeability is counteracted by dilation in fractures due to elevated pore pressures and reduced effective stress (Palmer and Mansoori, 1998).

The presence of water in cleat/micropores may also change its mechanical and chemical interaction. There are three types of water forms present in the organic portion of coal, namely, free water, bound water and non-freezing water (Norinaga et al., 1997). The water present in the coal matrix which does not crystallize under subzero conditions is referred as non-freezing water (Norinaga et al., 1997; Unsworth et al., 1988). Presumably, they influence gas transport differently. Free water may inhibit the flow of gas by blocking cleats and external surfaces, while bound water may reduce the adsorption capacity for sorbing gas in micropores. Moisture often swells coals and reduces adsorption capacity for CH_4 and CO_2 (Day et al., 2008; Joubert et al., 1974; Kelemen et al., 2006; Levy et al., 1997; Pan et al., 2010; van Bergen et al., 2009). The presence of elevated water content is thought to reduces the sorptive capacity of CH_4 and CO_2 by plugging the microstructures (Levine, 1991; Pan and Connell, 2012) reducing capacity and the extent of sorption-induced swelling. However, the bulk water can hold dissolved CO_2 increasing its capacity (Chikatamarla et al., 2009). The moisture in coal is dependent on the rank, oxygen functionality, and pore size distribution/fracture network. This can vary widely over the rank, for example, Australian lignite coals often containing up to 60% moisture by mass with much lower values for bituminous coals (Durie, 1991). The bulk water present in the meso-and macropores/fractures may significantly influence the permeability. While, the bound water associated with the oxygen functionality of the coal often in micropores may influence the gas capacity. Moisture in the micropores is thought to be particularly important in the blocking of access to CO_2 gas to the preferential sorption sites (Prinz and Littke, 2005; Radlinski et al., 2009). The moisture content reduces the capacity of CH_4 in bituminous coal up to a critical point, with additional moisture having little effect (Joubert et al., 1973, 1974).

Coal permeability is also a function of net effective stress (Brace et al., 1968; Gash et al., 1993). Cleat closure can occur with increasing effective stress resulting in the closure of smaller cleats, and a reduction in permeability as the interconnections between pores and cleats are reduced (Soeder, 1991). Empirical relationships between permeability and effective stress have been proposed (Bai et al., 1995; Durucan and Edwards, 1986; Min et al., 2009; Seidle et al., 1992; Somerton et al., 1975) including the role of stress cycling on permeability loss (Harpalani and Chen, 1995; Somerton et al., 1975).

Given the complexity of the processes various models have been suggested to predict permeability transformations. These models may be divided into analytical and numerical coupled flow models (Palmer, 2009). Analytical models are further divided into stress based (Bai et al., 1993; Durucan and Shi, 2009; Liu et al., 2010a; Palmer, 2009; Palmer and Mansoori, 1998; Pan et al., 2010; Shi and Durucan, 2005, 2008) and strain based (Clarkson et al., 2010; Gu and Chalaturnyk, 2006; Harpalani and Chen, 1995; Levine, 1996; Liu et al., 2010b, 1997; Ouyang and Elsworth, 1993) models. Until recently, most models described the permeability empirically as a function of sorption induced swelling and effective stress. Such analytical models are simple, easy to use with acceptable accuracies and have demonstrated acceptable fits for San Juan basin methane production data. However, the understanding of cumulative or lumped effect of physical processes (sorption induced swelling, effective stress and moisture-influenced swelling effects) remains limited. Coupled flow models have received increased attention because of their ability to deconvolve important first order processes that contribute to permeability evolution (Gu and Chalaturnyk, 2005; Liu and Rutqvist, 2010; Liu et al., 2010b, 2011; Mazumder and Farajzadeh, 2010; Pan and Connell, 2007; Pan et al., 2010; Robertson and Christiansen, 2007; Siriwardane et al., 2009; Wu et al., 2010a, b, c), but unfortunately the processes are not well constrained.

In this work the evolution of permeability is explored for Uinta basin bituminous coal to account for the important first order effects of effective stresses, gas pressure, and moisture content on permeability evolution. These characterizations are constrained by laboratory observations, fit to appropriate mechanistic models (Izadi et al., 2011; Min et al., 2009) and applied to the optimized recovery of CH_4 from coalbeds under CO_2 injection during ECBM recovery.

2. Experimental methods

We complete forced fluid percolation experiments on eight cylindrical samples stressed to in situ conditions. These experiments use He, CH_4, CO_2 as permeants and allow the role of swelling on the dynamic evolution of permeability to be examined.

2.1. Samples

A block sample of coal was collected from an underground coal mine from the subbituminous/bituminous region of the Uinta basin (Colorado, USA). The calorific value of this coal on a dry basis was 12000 BTU/lb (ASTM D388, 2005). The fixed carbon, volatile material and ash yield on the dry basis were determined as 56.99%, 38.31% and 4.70% (ASTM D7582, 2010) indicating bituminous rank. Eight cylindrical core samples of 2.5 cm diameter and 5 cm length were sampled horizontally (into the bedding plane) from immediately adjacent lithographic similar sites. The natural fracture network (butt and face cleats) had approximately uniform spacing in these samples (~10 mm). Moisture content, defined as the mass of water present per mass of coal, was 5% by mass for the as-received sample (ASTM, 2010). Porosity of the as-received sample, including the fracture and cleat network, was 16% using He as the injecting fluid. The methane sorption capacity of dry coal core under 10 MPa of constant confining stress was 0.12 mmol/g. Two samples were kept in a vacuum at 70 °C for a few hours followed by immersion in 105 °C dry air for an hour to achieve lower moisture contents. Cleats within the other samples were pre-saturated by flow-through of moisture for 24 h at a rate 0.1 ml/s prior to emplacement into a humidifier containing a saturated solution of K_2SO_4 to maintain 97% relative humidity (ASTM, 2007). Six samples were left in the desiccators for few months (1–4) at 40 °C, depending on the desired moisture content (up to ~9% by mass). The moisture content in each core was determined from the

Table 1
Suite of variables and prescribed ranges utilized in the experiments, for gas pressure P_p, permeability k, axial stress σ_1, confining stress σ_3, and axial strain ε_a.

Experimental variables	Experimental range	Measured outputs
Temperature	Constant	N/A
Gas pressure	1–8 MPa	P_p
Moisture content	Dry (1%) to moist (9%)	N/A
Axial stress σ_1	10 MPa	σ_1
		σ_3
Confining stress σ_3	10 MPa	ε_a
Gas type	He, CO_2, CH_4	N/A

core-cuttings taken from the core prior to the experiments and assumed to be the representative of the volumetric moisture content. Moisture equilibrated cores were used immediately, other cores were kept in laminated argon-filled bags to limit deterioration (Glick et al., 2005). The samples were wrapped in aluminum foil before loading into the permeability cell to prevent any adsorption or diffusion (of CO_2 and CH_4) through the rubber jacket during the permeability experiments. The absence of leakage and external adsorption was confirmed by the constant equilibrium pressure profile after pulse test.

2.2. Apparatus

Experiments were completed using a simple triaxial apparatus capable of applying defined effective stress paths and concurrently measuring permeability and sortive capacity (Fig. 1). All experiments were performed in a 'free expansion/shrinkage under constant stress' mode. The apparatus comprises a tri-axial cell to confine the sample at prescribed stresses, an axial strain gauge to monitor the shrinkage or swelling in the axial direction, ISCO syringe pumps to apply stresses and to measure volume strains (axial and confining), pressure transducers to monitor the upstream and downstream reservoir pressures and a data acquisition system (DAS). The volumes of the upstream and downstream reservoir were 17.36 and 3.1 cm^3 respectively. Additional details of the equipment are described elsewhere (Wang et al., 2011). Pumps, transducers, strain gauges and reservoir volumes were calibrated prior to the experiments. A transient pulse test method (described in Section 2.4) was used to determine the permeability of the samples. The volumes of the reservoirs are significantly higher than the total adsorption capacity of the coal cores used in the experimental suites. Pulse test gas reservoirs were kept in a water-bath at room temperature ($\sim$20 °C) to avoid rapid temperature fluctuations. The temperature was assumed to be constant for the duration of each pressure pulse (<30 min.). Evenly grooved end-platens enforce uniform flow in the specimen during flow tests. Permeability was evaluated from the rate of pressure decay/gain in the upstream/downstream reservoirs (Brace et al., 1968) assuming no sorption during the short duration (<30 min) pulse decay experiments where the effective diffusion from the cleats would reach of the order of 0.1 mm into the 5 mm cleat blocks. System was calibrated and tested against known permeability sandstones Berea ($\sim$300 md) and Crab Orchard ($\sim$0.01 md).

2.3. Procedures

Coal cores were placed within the triaxial core holder and stresses were applied. A suite of experiments was conducted to identify the critical ECBM processes. Table 1, provides the ranges of experimental variables and measured outputs. Experiments were completed to explore the role of gas pressure, effective stress and moisture content on the evolution of permeability for sequential sweeps of He, CH_4 and CO_2. The following experimental sequence

was adopted for a given sample under constant isotropic stress with incremental gas pressures:

1. *He permeability*: He was circulated in the sample to measure baseline permeability. Here He has been considered as a non-adsorbing fluid, which is consistent with the majority of the literature.
2. *CH_4 permeability*: The sample was exposed to a predetermined pressure of CH_4 and saturation was assumed to have been achieved when the pressure transducer reading plateaued with time. The Typical time taken to achieve majority of saturation is $\sim$4 h. Permeability was then measured by pulse test at different gas pressures (2–8 MPa).
3. *CO_2 assisted sweep of CH_4*: The sample was sealed at the completion of step (2) and permeability was measured with the upstream reservoir charged with CO_2 and the downstream reservoir evacuated. This represents the process of ECBM recovery and explores the competitive exchange CO_2 for CH_4. At completion the gas mixture ($CO_2 + CH_4$) was released from the system.
4. *CO_2 permeability*: The sample was vented for 12 h aided by a mild vacuum ($\sim$25 mm Hg). The desorbed sample was resaturated by CO_2 and permeability was measured.
5. *He permeability*: The sample was vented to atmospheric pressure for 12 h followed by mild vacuum. The time allowed for CO_2 venting (three times of the saturation time) prior to He injection was deemed to be sufficient to remove majority of CO_2 from step 4. Then, He is recirculated through the sample to measure post-sweep permeability.

The removal of gas is required to reuse the coal core for the next permeability test in the experimental sequence. Here it may be noted that the pulse decay is not likely to result in the loss of significant moisture due to small gas-volume used for injection. The treatment used for removing the gases may have had some effect on moisture content of the coal. However, the moisture is more likely to be retained in the matrix due to its higher affinity. We do not quantify the retained gas sorption for various gases in this work. The comparison of the initial He permeability to the permeability following sorption and removal of CH_4 and CO_2 shows similar trends but with a lower permeability ($\sim$20%) indicating a combination of moisture retention that was desirable and some undesirable CO_2 retention hence the order of experimentation was kept as noted above.

All experiments were conducted at a mean total stress of 10 MPa (equivalent to and effective stress at $\sim$1000 m or $\sim$3500 feet depth). The evolution of permeability is measured under the influence of: (i) effective stress, (ii) gas pressure and (iii) water content (S_w).

2.4. Analysis

Coal permeability was evaluated by the transient pulse test method (Brace et al., 1968). In a typical run, a coal core was packed and placed under axial and radial stress in the triaxial apparatus as shown in Fig. 1. A mild vacuum was applied to evacuate the air from the sample reservoir system. The core was saturated with gas (He, CH_4 or CO_2) to an equilibrium pressure before applying a pressure pulse. A pressure pulse is allowed to flow through the core from the upstream reservoir to the downstream reservoir until the pressure reaches equilibrium, i.e. upstream and downstream pressures are approximately equal. This equilibrium pressure has been referred to as gas pressure. The pressure pulse is significantly smaller (<10%) than the initial gas pressure in the system. We have assumed that there is insignificant additional adsorption with less than 10% increment in gas pressure. The pressure loss in the upstream reservoir and pressure gain in the downstream reservoir are recorded with time. This process is repeated until the predetermined value of gas
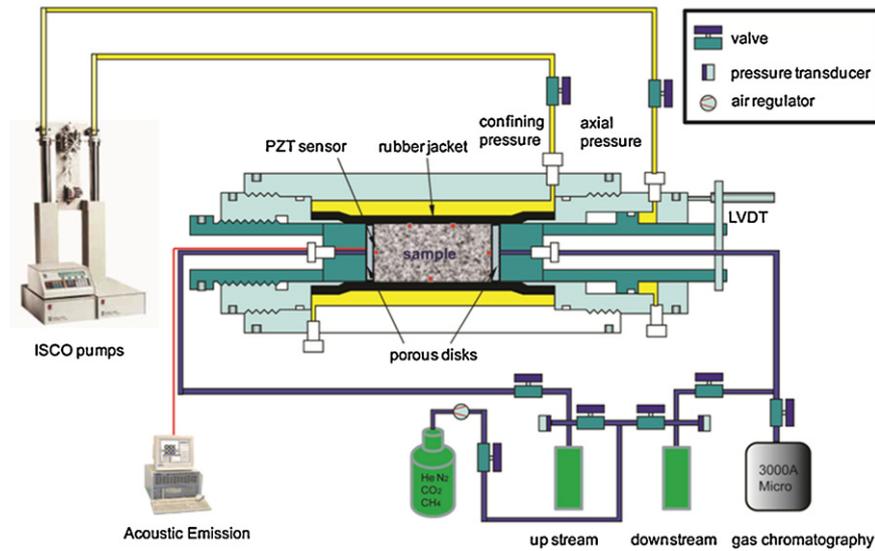
Fig. 1. Schematic of pulse test transient system.

pressure is achieved. The pressure–time profile from the experiment was used to obtain permeability, k (Brace et al., 1968).

$$k = \frac{\gamma \cdot \mu \cdot L_{up} V_{down}}{P_{eq} \cdot A \cdot (V_{up} + V_{down})} \tag{1}$$

where permeability k (m^2) is calculated from the decay parameter γ (s^{-1}) for a known gas viscosity μ (Pa.s) sample length L (m), equilibrium pressure at the end of the experiment P_{eq} (N/m^2) and cross sectional area of the specimen A (m^2) relative to upstream/downstream reservoir volumes $V_{up/down}$ (m^3), measured initial pressure $p_{up/down}$ (N/m^2) and transient upstream/downstream reservoir pressures $p_{up/down}$ (N/m^2).

$$\gamma = \frac{\log{(d(p_{up} - p_{down})/(p_{up^0} - p_{down^0}))_t}}{dt} \tag{2}$$

The value of γ is the slope of the line obtained from a $\log(d(p_{up} - p_{down})/(p_{up^0} - p_{down^0}))$ versus time straight line plot. This method yields a single value of permeability for a single pulse. Pressure-decay in the upstream reservoir and complementary pressure-gain in the downstream reservoir for a typical pulse test in moist coal with non-adsorbing (He) gas is shown in Fig. 2. Pulse-decay data
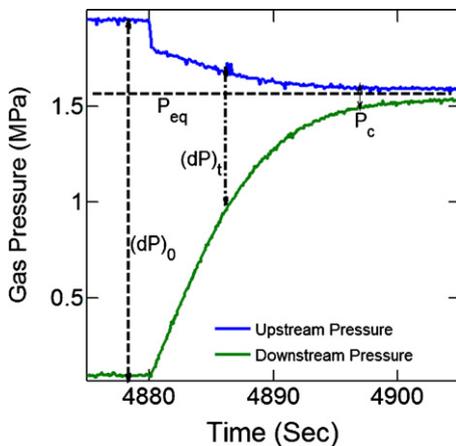
Fig. 2. Typical pressure-pulse decay in moist coal with non-adsorbing gas (Helium) during a transient pulse decay permeability test.

are reduced for $dP_o = p_{up} - p_{down}$, $dP_t = p_{up} - p_{down}$ and P_{eq}. A typical set of observations was used for the calculation of percentage error in the permeability. Uncertainties in measured pressure and length are ± 0.03 MPa and ± 0.01 mm respectively with a conservative assumption of 1% relative error in volume measurements. From these presumed errors, all values for permeability are accurate to within 9% determined conservatively for Eq. (1). Errors were calculated using an 'error propagation' method utilizing a Jacobian matrix (Wolfram Mathematica 7.2, 2009).

3. Results and discussions

Forced sequential injections of He, CH$_4$ and CO$_2$ were performed in coal cores at various moisture contents and gas pore pressures. Permeability was modulated by the effects of gas pressure, effective stress and moisture content. These three principal processes are further investigated below.

3.1. Influence of gas sorption

We record the evolution of permeability to sweeps of non sorbing He, and sorbing gases (CH$_4$ and CO$_2$). Permeability increased as the He gas pressure increased under constant confining stress (Fig. 3). This is consistent with the dilation of fractures as effective stresses reduce as gas pressures are elevated. Conversely, permeability was reduced for both CH$_4$ and CO$_2$, with increasing gas pressure with the reduction being more significant for CO$_2$ (Fig. 3). The reduction in permeability coincides with swelling strains. Presumably, observed dilational strains are the measured surplus strain after the interior closing of cleats has occured and resulted in net reduction of permeability even as effective stresses have reduced. For example, the permeability at 2 MPa is approximately six times of the minimum permeability observed at ~4 MPa in a 7% moisture saturated coal. The rate of change of permeability with pore pressure of sorptive gas (CH$_4$ or CO$_2$) is higher in dry coal in comparison to the moist coal (Fig. 3) as expected based on sorption capacity influences (Joubert et al., 1974). The water molecules have tendency to block the sorption sites for gases resulting in inhibited sorption of gas (Prinz and Littke, 2005). The reduction in adsorption decreases the rate of change of permability change with sorption as presented in Fig. 3. When either CH$_4$ or CO$_2$ desorbs by reducing gas
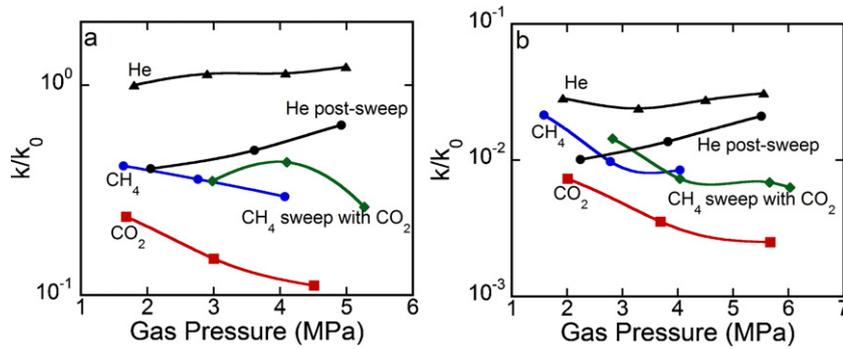
Fig. 3. (a) Evolution of permeability ratio with increasing pore pressure in a. partially dry (1–2% moisture content by mass) and b. for moist (7% moisture) coal. Computation error in the permeability values is within ±10%: $k_0 = 5.44 \times 10^{-15}$ m².

pressure then the permeability partly recovers to the baseline permeability ($k/k_0 \sim 1$) (not shown in Fig. 3). Note that k_0 has a value of 5.44×10^{-15} m². However this recovery was limited by the rate of desorption of the gas from the matrix blocks and into the fractures. Much of the original He permeability was retained in the sample implying that the core moisture content has not varied significantly during the experimental suite.

3.2. Influence of effective stress

There was an increase in permeability with increased gas pressure of He at constant confining stress for (1%, 5%, 7% and 9% by mass) moisture saturated coals (Fig. 3). This is consistent with the closure of microfractures as effective stresses increase. Conversely, for the moderately sorbing CH_4 and more strongly sorbing CO_2, the permeability decreases with an increase in gas pressure. This is the result of the dominant swelling response of the coal relative to the inhibited dilation due to decreased effective stresses at gas pressures below the pressure at which maximum swelling strain occurs. Interestingly, for various moisture content level coals, permeability ratios follow similar trends under constant confining stress and varying gas pressures (Fig. 3). For non-sorbing He, permeability was dominated by the effective stress response while for sorbing gases, the role of swelling was more prominent.

3.3. Influence of moisture content

The permeability of bituminous coal decreases with an increase in moisture content of the coal. Moisture contents varying from 1 to 9% by mass have been considered for this study. Samples with the higher moisture contents exhibit the lowest permeability with the injection of sorbing or non-sorbing gas (Fig. 3). The presence of moisture in fractures will inhibit the flow of gas by occluding pore-space. Additionally, the moisture in the micro- and meso-pores will influence flow tortuosity and out compete for sorption sites (Day et al., 2008; Fry et al., 2009). The moisture loading in coal swells the matrix to a degree (Fry et al., 2009; Robertson, 2005). Water occupying the fracture system is not expected to result in significant swelling while water in the matrix is more likely to result in matrix swelling depending on the pore size distribution. Presumably, the swelling developed in the matrix decreases the fracture aperture that further reduces the permeability. Shrinkage measurements on the Argonne suite show that the contraction of powdered coal on drying can range from 34 to 8% (Kelemen et al., 2005). The volumetric strains induced by moisture loading in bituminous/subbituminous coal blocks are in the same order of magnitude (~5%) (Fry et al., 2009) with low-rank having potentially much higher strains 12% (Czerw, 2011). The differences between the permeabilities to He, CH_4, CO_2-sweep and CO_2 are reduced most

significantly in the moist coal (7% moisture content) relative to the dry coal (1% moisture content) (Fig. 3). These observations are consistent with inhibited swelling in the moist coals (van Bergen et al., 2009). The presence of moisture in coal reduces the diffusion coefficient, ultimate adsorption capacity and sorption-induced swelling by gas (Day et al., 2011; Pan et al., 2010). Hence the reduction in permeability for dry coals is much higher than that of the moist coals (compare Fig. 3a and b). This is consistent with observations for bituminous coal (Wang et al., 2011). In the case of a constant head permeability test, an increase in permeability is expected in the moist coal experiments as the coal continues to dry with the flow of large volumes of various gases (Mathews et al., 2011). However, the transient pulse test approach minimizes this moisture loss over the more invasive fluid flow testing approaches and helps retain the integrity of the sample.

3.4. Mechanistic model

Observations of permeability evolution were used to develop a mechanistic model for permeability evolution in stress-constrained coal. As in the other experimental (Han et al., 2010) studies the cleat permeability is orders of magnitudes higher than the matrix permeability. We consider a model where individual cleats of finite length are embedded within a coal matrix (Izadi et al., 2011) and the processes (sorption/desorption) resulting in swelling/shrinkage occurring in the matrix directly affect the cleat permeability by changing the cleat aperture (Izadi et al., 2011; Wang et al., 2012). The rock-bridge model is based on matrix–fracture interaction (Izadi et al., 2011). This model was used to explore the changes in porosity and permeability that accompany gas sorption under conditions of constant applied stress and for increments of applied gas pressure. The influence of gas pressure, effective stress, and moisture content were evaluated to separately identify the individual effects on permeability. A single parameter was varied while other parameters being held constant. This approach allowed addressing the important aspects of permeability evolution.

3.4.1. Gas sorption

The permeability evolution data were fit to a model representing the evolution of permeability on coals subjected to prescribed stress boundary conditions (Izadi et al., 2011). This model identifies the change in permeability in the swelling regime.

The dynamic permeability of a cracked system may be represented as:

$$\frac{k}{k_0} = \left(1 + \frac{\Delta b}{b_0}\right)^3 \tag{3}$$

If external boundaries have zero displacement, the swelling strain is defined as:

$$\varepsilon_v = \frac{\Delta b \cdot a}{s \cdot s} \tag{4}$$

Volumetric strain due to swelling ε_v may be expressed as Langmuir type curve (Robertson, 2005):

$$\varepsilon_v = \varepsilon_L \frac{P}{P+P_L} \tag{5}$$

Using Eqs. (4) and (5), the relative aperture change may be calculated as:

$$\frac{\Delta b}{b_0} = \left(\frac{\varepsilon_L s^2}{ab_0} \right) \frac{P}{P+P_L} \tag{6}$$

Combining Eqs. (3) and (5), the change in permeability may be recovered as:

$$\frac{k}{k_0} = \left(1 + \frac{\Delta b}{b_0} \right)^3 = \left(1 + \left(\frac{\varepsilon_L s^2}{ab_0} \right) \frac{P}{P+P_L} \right)^3 \tag{7}$$

If an arbitrary variable C is such that

$$C = \left(\frac{\varepsilon_L s^2}{ab_0} \right) \tag{8}$$

then Eq. (7) may be rewritten as:

$$\frac{k}{k_0} = \left(1 + C\frac{P}{P+P_L} \right)^3 \tag{9}$$

where permeability k, initial permeability k_0, initial fracture aperture b_0, change in fracture aperture Δb, fracture length a, fracture spacing s, volumetric strain ε_v, peak Langmuir strain ε_L, gas pressure p, Langmuir pressure p_L and assumed fitting constant $C = (\varepsilon_L s^2 / ab_0)$ define the response. Here peak Langmuir strain is defined as the maximum strain that occurs due to gas adsorption at infinite pressure (Robertson, 2005). It may be noted that the parameter 'C' represents lumped response of swelling induced strain by both moisture and sorptive gas. Although, it is desirable from a scientific point of view to deconvolve the individual effect of moisture and sorption (CH_4 and CO_2) induced strain on permeability, we have specifically chosen not to separate the two components. This is for two reasons: first, to avoid increasing the number of free parameters in the model and second since it is non-trivial to separate the effect of moisture and gas-induced strain as the presence of moisture also influences the gas capacity hence the magnitude of swelling.

This formulation allows the evolution of normalized permeability to be represented by the analytical curves of (Fig. 4) where the magnitudes of C are evaluated from the best fit as indexed by the coefficient of correlation (R^2). These identify acceptable fits in the swelling dominant region for CH_4, CH_4-swept with CO_2 and for uptake of CO_2.

3.4.2. Effective stress

Many permeability models or empirical correlations index permeability as a function of effective stress (Durucan and Edwards, 1986; Jasinge et al., 2011; Somerton et al., 1975). We note (Fig. 5a) the log-linear trend in permeability with effective stress with a goodness of fit of 99%, supported by similar observations for various coals (Jasinge et al., 2011). This correlation may be represented as:

$$\frac{k}{k_0} = \alpha e^{-\beta \sigma'} \tag{10}$$

where permeability k, initial permeability k_0, effective stress σ' = confining stress – pore pressure, and the arbitrary material-specific constants α and β define response.

The slope of the permeability versus effective stress response line β (MPa^{-1}) represents the inverse of Young's modulus. The comparison of permeability evolution in dry and moist coals indicates that dry coals have higher modulus than moist coals (Fig. 5a). This means that the dry coals are less sensitive to effective stress compared to moist coals (Fig. 5a). Permeability decreases by two orders of magnitude with an increase in effective stress from 4 to 8 MPa in the moist coals. It is clear from Fig. 5a that permeability decreases with an increase in effective stress for the dry coal but that the magnitude of this decrease is much smaller than that of the other higher moisture saturated coal. The Young's modulus decreases as the moisture content increases in Australian bituminous coals which indicates coal hardening when losing moisture content (Pan et al., 2010). Alternatively, coal becomes less stiff with addition of moisture. The decrease in stiffness results in a greater sensitivity of aperture change to the applied stress and thereby a greater sensitivity of permeability change to stress change (Ouyang and Elsworth, 1993). The slope of the permeability–effective stress linear relationship is greater in moist coals than the dry coal (Fig. 5a), which indicates that the coals at higher moisture contents are less stiff. The permeability evolution data for high moisture content coal show scatter at higher effective stresses suggesting the existence of a lower-bound value of permeability. However, as observed, the coal samples with lower moisture content do not show this behavior at least in the range of 9 MPa. The lower-bound permeability values correspond to the scenario when fracture aperture reaches a threshold and does not change further with effective stress (Min et al., 2009). These values however seem to be dependent on moisture content of coal as shown by dotted line in the Fig. 5a.

3.4.3. Moisture content

Permeability evolution for the infiltration of He gas was observed to be log-linear with moisture content. An exponential decrease in permeability is observed with increasing moisture content of the coal (Fig. 5b). The decrease in He permeability may be as high as ~100 fold if the moisture content is increased from 1 to 9% (Fig. 5b). It is important to note that only non-adsorbing gas holds a log-linear relationship with increasing moisture content (Fig. 5b). We explain this behavior on the basis of coal fracture-wall swelling (Day et al., 2011, 2008) and the occlusion of micropores (Day et al., 2008) by the water molecules. The infiltrating water first occupies high energy water adsorption sites (Busch and Gensterblum, 2011) and the ease of access to a suitable-site for water-molecules becomes exponentially more difficult (Menon et al., 1991). Presumably, the water molecules then begin occupying free space in the matrix and the fracture when the majority of the adsorption sites are filled. This process reduces effective space allowing the flow of the injected gas. Hence, the exponential reduction in permeability is observed with the loading of moist in coals (Chikatamarla et al., 2009). Typical correlations shown in Fig. 5b may be represented as:

$$\frac{k}{k_0} = \gamma e^{-\delta S_w} \tag{11}$$

where permeability k, initial permeability k_0, moisture content S_w and the arbitrary coal characteristics constants γ and δ define behavior. The higher values of parameter δ indicate a greater sensitivity to interaction between coal and a particular gas in the presence of moisture. The moist coals swell less than dry coals in the presence of a sorbing gas. However, the moist coals show lower permeability than the dry coal because of the cumulative effect of moisture and of the sorbing gases.

3.5. Parameter optimization

The prior observations and characterizations were used to describe a phenomenological model for the combined response to
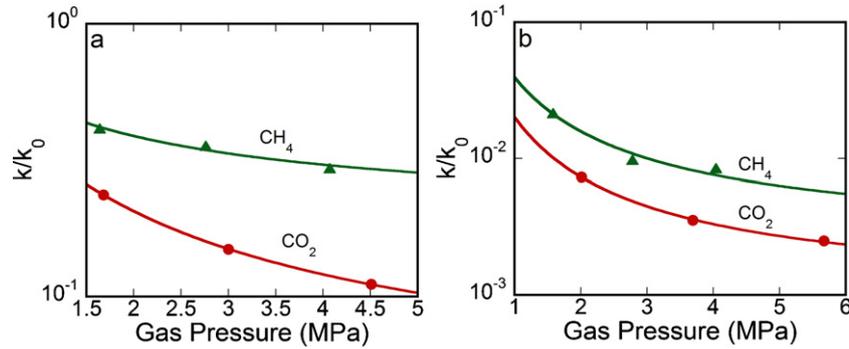
Fig. 4. Analytical fits of Eq. (9) to the measured permeability evolution for (a) dry (1% moisture) and (b) moist (fracture saturated) coal. R^2 fit for all curves are >90%.

stress, gas pressure and moisture content. The evolution of permeability may be represented by the superposition of individual processes as:

$$\frac{k}{k_0} = f(\sigma', p_g, S_w) \qquad (12)$$

where effective stress σ' and moisture content S_w are as previously defined and p_g is the pore pressure of gas (CH_4, CO_2, He). The change in aperture of the fracture largely results from a change in effective stress and sorption induced swelling as shown in Fig. 6. The term $e^{-\delta S_w}$ represents the occluding effect of moisture is a pre-factor for both effective stress and gas pressure and its presence can either enhance or depress the magnitude of the two above mentioned processes. Therefore, the cumulative effect can be represented as the sum of sorptive-swelling and stress-dilatational effects and the product of these two concurrent influences with the influence of moisture content (Fig. 6). This is further explained in Fig. 6. When stress is applied to the coal (Fig. 6a) the aperture of the fracture reduces (Fig. 6b). For a sorptive gas injected into the fracture under constant confining stress condition, the aperture is further reduced by inducing swelling (Fig. 6c). The increase in moisture content further magnifies the reduction in permeability which may be due to the occlusion of the pores and the change in Young's modulus of the matrix. Mathematically, this can be represented as:

$$\frac{k}{k_0} \propto (\text{effective stress} + \text{sorption induced swelling})$$
$$\times \text{moisture occluding effect} \qquad (13)$$
$$\frac{k}{k_0} = \left\{ \left(1 + \frac{C \cdot p}{p + P_L} \right)^3 + e^{-\beta \sigma'} \right\} \times e^{-\delta S_w}$$

MATLAB® curve fit toolbox was used to optimize the values of the parameters (C, P_L, β and δ). This function utilizes the lsqcurvefit

algorithm to find the best possible set of values under prescribed constraints (MATLAB Curvefit Toolbox, 2009).

Permeability reduces as the coal swells reducing fracture aperture with increasing gas pressure of the sorbing gas. As the peak Langmuir strain is approached, the reduction in permeability halts and permeability increases linearly with gas pressure (Fig. 7). The reduction in permeability ranges from 5 to 10 folds depending on the gas injected (Fig. 7). A regain in permeability was observed at sufficiently high gas pressures. For instance, the CH_4 permeability in the 7% moisture saturated coal decreases by ~200% as gas pressure increases from ~1.5 to ~4.1 MPa. The coal regains its original permeability as gas pressure is further increased to ~6.2 MPa. The reduction in permeability is 40 fold for CH_4 and 60 fold for CO_2 in moist coal (7% moisture content) with respect to dry coal (Fig. 7). The rate of permeability loss is controlled by crack geometry (Izadi et al., 2011), the Langmuir swelling strain ε_L and the void "stiffness" β. However, the rate of permeability increase is controlled by crack geometry and void "stiffness" alone. The permeability evolution may be approximated by a single non-dimensional variable incorporating fracture spacing, fracture-length, Langmuir strain, and initial permeability. Here Langmuir strain is defined as the swelling induced strain in coal at certain gas pressure. The swelling increases and the permeability decreases with an increase in gas pressure of the sorbing gas (Fig. 7a and b, Region I). We eliminate the possibility of the Klinkenberg effect as the size of cleats (~0.5 mm) is significantly higher than the mean free path of the gas used (~0.3 nm). Therefore, the decrease in permeability in Region I can only be attributed to sorption induced swelling. However, permeability increases as the pressures of the infiltrating gas becomes approximately equal to the pressure at which maximum adsorption occurs.

This model represents the principal features of permeability evolution in swelling media and is a mechanistically consistent and plausible model for behavior. The proposed model tracks the role
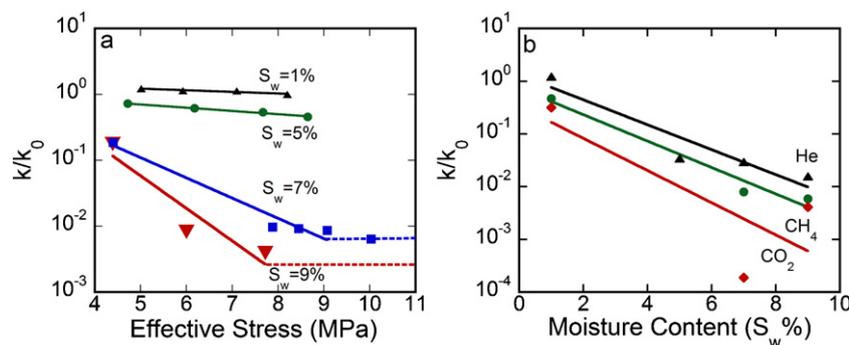
Fig. 5. Analytical fits to the measured permeability evolution. (a) Evolution in permeability with effective stress (Eq. (10)) for Helium permeability and (b) evolution of permeability with moisture content (Eq. (11)) in coal. R^2 fit for all curves are 99% except CO_2.
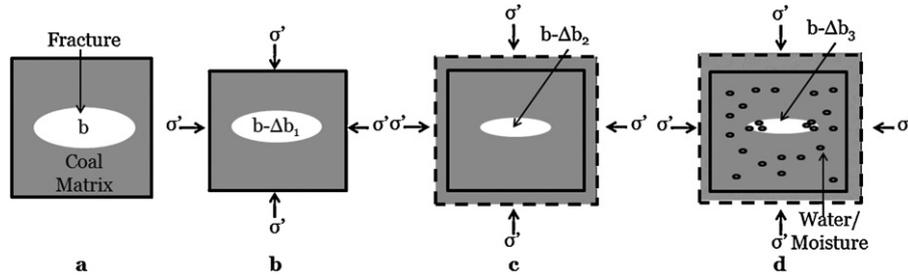
Fig. 6. Representation of mechanistic processes interplaying simultaneously in ECBM. (a) A unit of coal-fracture system. (b) Reduction in aperture 'b' by 'Δb_1' on application of stress. (c) Reduction in aperture by 'Δb_2' due to sorption induced swelling in stress-constrained unit. (d) Reduction in aperture by 'Δb_3' due to moisture infiltration. Here $\Delta b_1 < \Delta b_2 < \Delta b_3 < \Delta b_4$.
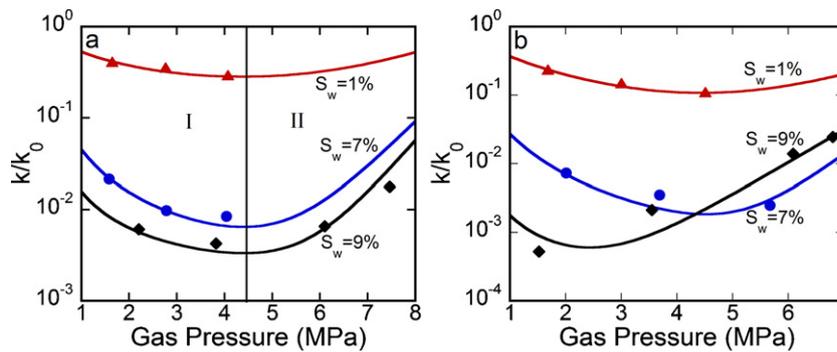
Fig. 7. Analytical fits to the Eq. (13) for the observations of permeability evolution with (a) CH_4, (b) CO_2 at various moisture-content of coals. Region I is swelling dominant and Region II effective stress dominant.

of gas pressure, effective stress and moisture content on the evolution of permeability in coal. To the best of our knowledge, no current permeability model accounts for the presence of moisture despite experimental evidence for the same.

3.6. Congruence of fit pattern with physical phenomenon

The fitting parameters for C, P_L, β and δ recovered as described previously are summarized in Table 2. These parameters may be described in terms of the physical processes they represent. In this section, we explore the appropriateness of these parameters relative to measured parametric magnitudes reported in the literature.

1. Parameter C. After rearranging Eq. (8), the Langmuir strain may be expressed as $\varepsilon_L = (Cab_0/s^2)$. Typical values of cleat spacing $s = 5$ mm, cleat width $a = \sim5$ mm, cleat aperture $b_0 = 1/2$ mm were obtained from the dry coal used in this work. The range of values for parameter C was obtained from Table 2. Eq. (8) yields the values of ε_L using typical values of s, a, b_0 and C. The Langmuir

strain ε_L varies in the range of 0.05–0.1 similar to magnitudes previously recorded (Day et al., 2011; Reucroft and Patel, 1986).
2. Parameter P_L. Langmuir pressures P_L vary in the range (2.0–0.1) MPa (Table 2). We observe that minimum permeabilities occur at $\sim$4.1 MPa (Fig. 7). Minimum permeability occurs at a pressure after which no additional sorption takes place. A shift of $\sim$1.8 MPa is observed in the case of CO_2 at 9% moisture content.
3. Parameter β. The parameter β, increases from 0.5 to 1.4 for moisture contents ranging from 1 to 9%. Dry coals are stiffer than the moist coals and as a result their permeabilities are less affected by changes ineffective stresses. These findings are consistent with the observations of others (White and Mazurkiewicz, 1989).
4. Parameter δ. The moisture induced offset δ of permeability is higher for CO_2 (1.88) than for CH_4 (1.1). This indicates that CO_2 has a higher impact on swelling even in the presence of moisture and retains molecular access those sites which remain inaccessible to moisture (Prinz and Littke, 2005). A plausible argument is that the transport of CO_2 to adsorption sites is easier because of the smaller kinetic diameter of the CO_2 molecule.

3.7. Model validation

The mechanistic model proposed in this paper has been validated using the CH_4 and CO_2 permeability evolution data reported on a water saturated Pennsylvanian Anthracite coal (Wang et al., 2011) and CO_2 permeability evolution data reported on a European high volatile bituminous coal (Pini et al., 2009).

The permeability evolution observed for CH_4 and CO_2 on naturally fractured coal samples from Northumberland basin in Pennsylvania (Wang et al., 2011) (Fig. 8) shows the normalized permeability evolution data for CH_4 and CO_2 under 6 MPa of constant confining stress. The normalizing factor used was the

Table 2
Typical value of the fit parameters in Eq. (13). See text for the definition of fit parameters.

Gas, S_w%	Fit parameters			
	C	P_L	β	δ
1. CH_4, 1	0.56	1.9	0.5	1.1
2. CH_4, 7	0.9	0.4	1.2	
3. CH_4, 9	0.89	0.2	1.4	
4. CO_2, 1	0.84	2	0.6	1.9
5. CO_2, 7	0.96	0.4	1.4	
6. CO_2, 9	0.96	0.1	1.1	
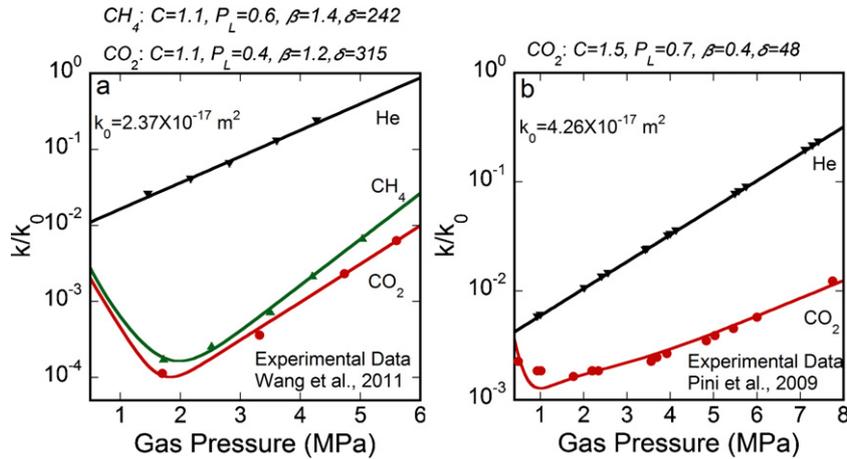
Fig. 8. Validation of proposed model against permeability evolution experimental data for (a) CH_4 and CO_2 as reported by Wang et al. (2011). (b) CO_2 as reported by Pini et al. (2009). The fitted model parameters are shown.

helium permeability of dry coal under no confining stress, i.e. k_0 (2.37×10^{-17} m^2). The goodness of fit for both CH_4 and CO_2 is greater than 99.8%, i.e. the trend predicted by the proposed model is in excellent agreement with the published data. The values of the fitting parameters are shown in Fig. 8a. The absence of adsorption and strain measurement data on Pennsylvanian Anthracite coal restricts us from any direct parametric comparison. However, we have compared our model fitting parameter values with those of coals of similar rank from other basins in the world. It is important to note that the literature values for Langmuir pressure (P_L) and Langmuir strain (ε_L) are reported for pulverized coal while our model derives these values based upon the permeability evolution data on cores. The Langmuir pressure P_L for CH_4 ($\sim$0.6 MPa) is of the same order of magnitude as those ($\sim$1 MPa) reported for powdered Chinese anthracite coal (Li et al., 2010). The model-driven Langmuir strain (ε_L) for CO_2 is 0.011 which is close to the reported value (0.028) for powdered anthracite coal (Walker et al., 1988). The different values for P_L and ε_L would yield different production characteristics. It may be noted here that the majority of the experimental data (Wang et al., 2011) fall in Region II, the region dominated by effective stress. However our permeability evolution data covers both Regions I and II although the majority is in Region I. The acceptable fits on experimental data in both regions using our proposed model suggest a broad, and perhaps a universal, applicability. Intuitively, when gas pressure approaches, zero (gauge pressure), then, for a given confining stress, the permeability to sorbing gases (CH_4 and CO_2) should be equivalent to that for the non-sorbing gases (He) as the null swelling and effective stress effects are all equivalent. This is expected because at zero pressure (vacuum), the effect of sorption (water, CH_4 and CO_2) on permeability is negligible. Although, the region below 0.5 MPa is not of practical interest for ECBM application, our initial extrapolation to zero pressure suggests a convergence in permeability of He in dry coal with the permeability of CH_4 and CO_2 in water saturated coal (Fig. 8).

The model has also been validated against permeability evolution data on CO_2 for a bituminous coal sample in both region I as well region II (Fig. 8b) (Pini et al., 2009). The model explains the data with a goodness of fit 98%. Also, we observe that the model-driven Langmuir pressure value P_L (0.7 MPa) agrees very well with the reported experimental value (0.8 MPa) for this coal. Additionally, both data sets from Wang et al. (2011) and Pini et al. (2009) though made on different samples, show a similar trend in convergence of He permeability with those of CH_4 and CO_2. These validations indicate the robustness of the proposed model despite variations in coal properties.

4. Lumped parameter model for ECBM optimization

Enhanced coalbed methane recovery with CO_2 injection operates by the preferential sorption of CO_2 in the coal matrix; CH_4 residing within the matrix desorbs as CO_2 is sorbed. We follow the evolution of the permeability of the coal with gas pressure of CH_4 and CO_2 as CO_2 is injected and CH_4 is recovered at upstream and downstream sites, respectively. The CH_4-permeability is higher than the CO_2-permeability in the dry to medium-moist coals for practical ranges of reservoir pressures (Fig. 9a). We plot the permeability evolution versus gas pressure curves using our mechanistic model presented in Eq. (13). Specifically, we explore the conditions required to ensure that permeability remains higher during CO_2 assisted ECBM than the initial permeability to CH_4. The conditions that ensure that both injection (CO_2) and recovery (CH_4) permeabilities remain higher than the initial reservoir (CH_4) permeability may be schematically represented as in Fig. 9a. Initial reservoir permeability at pressure P_r (assuming 100% CH_4) can be equal to the CO_2-permeability (assuming 100% CO_2 at the end of ECBM) at another pressure P_i (Fig. 9a).

$$k_{P_r}^{CH_4} = k_{P_i}^{CO_2} \qquad (14)$$

where initial reservoir permeability, $k_{P_r}^{CH_4}$ and permeability at the end of ECBM recovery, $k_{P_i}^{CO_2}$ describe the response. Pressures P_r and P_i may be solved-for numerically using Eq. (14). We use the permeability fitting parameters (Table 2) to explore two scenarios of initial reservoir pressures either under or above saturation pressures; though oversaturated reservoirs are the most common (Pashin, 2010; Pashin and McIntyre, 2003). Here, the pressure range below the pressure point at which the adsorption isotherm plateaus has been referred to as undersaturation region and the one above this pressure point as oversaturation region. It should be noted that the pressure point separating the under- and over-saturation regions itself is always greater than the Langmuir pressure P_L.

4.1. Undersaturated reservoir

If the initial reservoir pressure is lower than the pressure at which maximum adsorption occurs, then the reservoir should be initially depressurized to pressure P_i by withdrawing CH_4 (Fig. 9a). We calculate withdrawal/injection pressure P_i for an initial reservoir pressure P_r using Eq. (14). This scenario is represented as the 'withdrawal' region in Fig. 9. For an undersaturated reservoir, recovery of CH_4 will always increase the permeability at the recovery well and CO_2 injection can only retain the original permeability
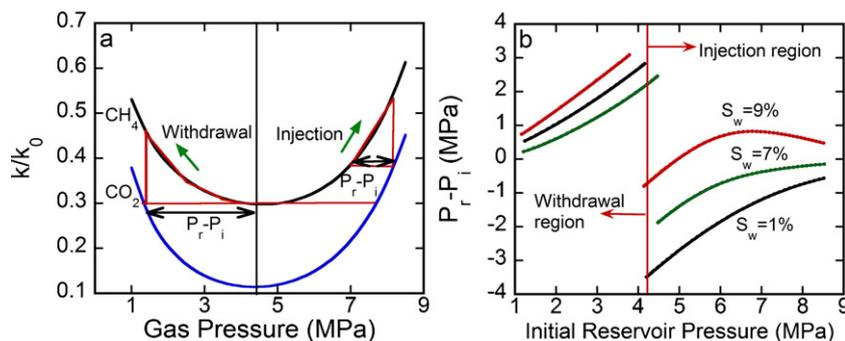
Fig. 9. Optimization of coalbed methane extraction while accommodating swelling induced permeability change. (a) Represents the CH_4 and CO_2 permeability at various pore pressures in dry coal. Withdrawal and injection regions are divided at the basis of Langmuir pressure. (b) The difference of the withdrawal/injection pressure and initial reservoir pressure.

or better if the injection pressure rises above the critical pressure and an additional amount defined by the nested CH_4–CO_2 permeability curves (Fig. 9a). This condition may be avoided if initial injection of a non-sorbing gas, for example N_2, is used as a substitute for CO_2.

This optimized injection schedule ensures that there is no reduction in permeability during ECBM recovery. Fig. 9b shows the necessary extent of initial depressurization ($P_r - P_i$) for any initial reservoir pressure for a variety of initial moisture contents in coal.

4.2. Oversaturated reservoir

If the initial reservoir pressure is greater than the pressure at which maximum adsorption occurs, then elevating reservoir pressure without the injection of sorbing gas is first required. This can be accomplished with the injection of non-adsorbing gas (e.g. N_2) would result in a higher permeability by moving up the CH_4 permeability curve (Schepers et al., 2010) (Fig. 9a). The injection of CO_2 should only follow when the reservoir gas pressure is above the required pressure obtained from Eq. (14). More CO_2 is adsorbed in the coal as the injection proceeds and at time $t = \infty$ (end of ECBM) maximum swelling would occur resulting in a minimum permeability value. The permeability at the end of this cycle is then guaranteed to be at least equal to that at the beginning of the ECBM process (Fig. 9a). The discontinuity in the pressure-permeability relations (Fig. 9b) at a pressure equal to the saturation pressure shows a demarcation line between the injection and withdrawal region.

For reservoirs initially at pressures above the saturation pressure then withdrawal pressures will reduce permeability unless the pressure change is sufficiently large to carry the reservoir through the critical pressure, identified as the permeability minimum at about the pressure where maximum adsorption occurs. For CO_2 injection the permeability at the injection well may be retained above the initial reservoir permeability if injection pressures are typically of the order of one to a few MPa above the critical reservoir pressure.

Both scenarios discussed above provide the basis to define the appropriate production pressures and their scheduling to optimally recover CH_4 using the injection of CO_2, but do not guarantee that breakthrough of CO_2 to the production well will not occur. This case requires a more involved analysis.

5. Conclusions

The permeability evolution in bituminous coal with injection of both sorptive and non-sorptive gases under mechanically constrained condition was investigated. Also, the effect of critical processes involved in ECBM recovery from coalbed reservoirs related to the evolution of permeability in bituminous coal was quantified. The following conclusions can be drawn from this study:

1. Measurement of permeability of a bituminous coal from the Uinta Basin showed that the permeability decreases with increasing pressure of the sorbing gas. This decrease may be as high as an order of magnitude for this coal. The reduction in permeability halts at a critical pressure corresponding to the point at which maximum adsorption is achieved and then increases as a consequence of diminishing effective stresses.
2. We confirm permeability to be dependent primarily on three processes: sorption-induced swelling, stress-induced cleat closure and pore occlusion due to the presence of moisture in coal. Further, the effect of each process on permeability evolution was quantified.
3. We confirm that the presence of moisture lowers net permeability compared to dry coal. The decrease in He permeability may be as high as ~100 fold if the moisture content is increased from 1 to 9%. This behavior is overprinted on the sorptive decrease in permeability, which are greater for $CO_2 > CH_4 > He$.
4. A mechanistic model was proposed which represents the permeability evolution under mechanically constrained conditions as effective stress, gas pressure and moisture content modulate behavior in the coal. Also, we showcase this model to explain the permeability evolution data published in the literature.
5. Two ECBM optimization scenarios representing both "undersaturated" and "oversaturated" reservoirs were identified based on the initial reservoir pressure. Additionally, we identify two ECBM optimization strategies which could prevent permeability loss during this process.

References

ASTM, 2007. D1412-07 standard test method for equilibrium moisture of coal at 96 to 97 percent relative humidity and 30 °C.
ASTM International, 2010. D3302/D3302M-10, standard test method for total moisture in coal.

ASTM D388, 2005. Standard classification of coals by rank. IHS, Pennsylvania, United States.

ASTM D7582, 2010. Standard test methods for proximate analysis of coal and coke by macro thermogravimetric analysis.

Bai, M., Elsworth, D., Roegiers, J.C., 1993. Modeling of naturally fractured reservoirs using deformation dependent flow mechanism. International Journal of Rock Mechanics and Mining Sciences and Geomechanics Abstracts 30, 1185–1191.

Bai, M., Roegiers, J.-C., Elsworth, D., 1995. Poromechanical response of fractured-porous rock masses. Journal of Petroleum Science and Engineering 13, 155–168.

Brace, W.F., Walsh, J.B., Frangos, W.T., 1968. Permeability of granite under high pressure. Journal of Geophysics Research 73, 2225–2236.

Busch, A., Gensterblum, Y., 2011. CBM and CO_2-ECBM related sorption processes in coal: a review. International Journal of Coal Geology 87, 49–71.

Bustin, R.M., Cui, X., Chikatamarla, L., 2008. Impacts of volumetric strain on CO_2 sequestration in coals and enhanced CH_4 recovery. AAPG Bulletin 92, 15–29.

Chikatamarla, L., Bustin, R.M., Cui, X., 2009. CO_2 sequestration into coalbeds: insights from laboratory experiments and numerical modeling. AAPG Studies in Geology 59, 457–474.

Chikatamarla, L., Cui, X., Bustin, R.M., 2004a. Implications of volumetric swelling/shrinkage of coal in sequestration of acid gases. In: International Coalbed Methane Symposium Proceedings, Tuscaloosa, AL.

Chikatamarla, L., Cui, X., Bustin, R.M., 2004b. Implications of volumetric swelling/shrinkage of coal in sequestration of acid gases. In: The International Coalbed Methane Symposium, Tuscaloosa, AL.

Clarkson, C.R., Pan, Z., Palmer, I., Harpalani, S., 2010. Predicting sorption-induced strain and permeability increase with depletion for coalbed-methane reservoirs. SPE Journal 15, 152–159.

Cui, X., Bustin, R.M., Chikatamarla, L., 2007. Adsorption-induced coal swelling and stress: implications for methane production and acid gas sequestration into coal seams. Journal of Geophysics Research 112, B10202.

Czerw, K., 2011. Methane and carbon dioxide sorption/desorption on bituminous coal—experiments on cubicoid sample cut from the primal coal lump. International Journal of Coal Geology 85, 72–77.

Day, S., Fry, R., Sakurovs, R., 2011. Swelling of moist coal in carbon dioxide and methane. International Journal of Coal Geology 86, 197–283.

Day, S., Fry, R., Sakurovs, R., Weir, S., 2010. Swelling of coals by supercritical gases and its relationship to sorption. Energy and Fuels 24, 2777–2783.

Day, S., Sakurovs, R., Weir, S., 2008. Supercritical gas sorption on moist coals. International Journal of Coal Geology 74, 203–214.

Durie, R.A., 1991. The Science of Victorian Brown Coal: Structure, Properties, and Consequences for Utilization. Butterworth-Heinemann.

Durucan, S., Edwards, J.S., 1986. The effects of stress and fracturing on permeability of coal. Mining Science and Technology 3, 205–216.

Durucan, S., Shi, J.-Q., 2009. Improving the CO_2 well injectivity and enhanced coalbed methane production performance in coal seams. International Journal of Coal Geology 77, 214–221.

EPA, 2004. Evaluation of impacts to underground sources of drinking water by hydraulic fracturing of coalbed methane reservoirs—final report, p. 424.

Fry, R., Day, S., Sakurovs, R., 2009. Moisture-induced swelling of coal. International Journal of Coal Preparation and Utilization 29, 298–316.

Gash, B.W., Volz, R.F., Potter, G., Corgan, J.M., 1993. The effect of cleat orientation and confining pressure on cleat porosity, permeability and relative permeability in coal. In: International Coalbed Methane Conference, University of Alabama, Tuscaloosa, AL, pp. 247–255.

Glick, D.C., Mitchell, G.D., Davis, A., 2005. Coal sample preservation in foil multilaminate bags. International Journal of Coal Geology 63, 178–189.

Gu, F., Chalaturnyk, R.J., 2005. Analysis of coalbed methane production by reservoir and geomechanical coupling simulation. Journal of Canadian Petroleum Technology 44, 33–42.

Gu, F., Chalaturnyk, R.J., 2006. Numerical simulation of stress and strain due to gas sorption/desorption and their effects on in situ permeability of coalbeds. Journal of Canadian Petroleum Technology 45, 52–62.

Han, F., Busch, A., van Wageningen, N., Yang, J., Liu, Z., Krooss, B.M., 2010. Experimental study of gas and water transport processes in the inter-cleat (matrix) system of coal: anthracite from Qinshui Basin, China. International Journal of Coal Geology 81, 128–138.

Harpalani, S., Chen, G., 1995. Estimation of changes in fracture porosity of coal with gas emission. Fuel 74, 1491–1498.

Izadi, G., Wang, S., Elsworth, D., Liu, J., Wu, Y., Pone, D., 2011. Permeability evolution of fluid-infiltrated coal containing discrete fractures. International Journal of Coal Geology 85, 202–211.

Jasinge, D., Ranjith, P.G., Choi, S.K., 2011. Effects of effective stress changes on permeability of Latrobe valley brown coal. Fuel 90, 1292–1300.

Joubert, J.I., Grein, C.T., Bienstock, D., 1973. Sorption of methane in moist coal. Fuel 52, 181–185.

Joubert, J.I., Grein, C.T., Bienstock, D., 1974. Effect of moisture on the methane capacity of American coals. Fuel 53, 186–191.

Kelemen, S.R., Kwiatek, L.M., Lee, A.G.K., 2006. Swelling and sorption response of selected Argonne Premium bituminous coals to CO_2, CH_4, and N_2. In: International Coalbed Methane Symposium, Tuscaloosa, AL, USA.

Kelemen, S.R., Kwiatek, L.M., Siskin, M., Lee, A.G.K., 2005. Structural response of coal to drying and pentane sorption. Energy and Fuels 20, 205–213.

Kiyama, T., Nishimoto, S., Fujioka, M., Xue, Z., Ishijima, Y., Pan, Z., Connell, L.D., 2011. Coal swelling strain and permeability change with injecting liquid/supercritical CO_2 and N_2 at stress-constrained conditions. International Journal of Coal Geology 85, 56–64.

Levine, J.R., 1991. The impact of oil formed during coalification on generation and storage of natural gas in coal bed reservoir system. In: 3rd Coalbed Methane Symposium Proceedings, Tuscaloosa, AL.

Levine, J.R., 1996. Model study of the influence of matrix shrinkage on absolute permeability of coal bed reservoirs, vol. 109. Geological Society, London, pp. 197–212 (Special Publications).

Levy, J.H., Day, S.J., Killingley, J.S., 1997. Methane capacities of Bowen Basin coals related to coal properties. Fuel 76, 813–819.

Li, D., Liu, Q., Weniger, P., Gensterblum, Y., Busch, A., Krooss, B.M., 2010. High-pressure sorption isotherms and sorption kinetics of CH_4 and CO_2 on coals. Fuel 89, 569–580.

Liu, H.-H., Rutqvist, J., 2010. A new coal-permeability model: internal swelling stress and fracture–matrix interaction. Transport in Porous Media 82, 157–171.

Liu, J., Chen, Z., Elsworth, D., Miao, X., Mao, X., 2010a. Evaluation of stress-controlled coal swelling processes. International Journal of Coal Geology 83, 446–455.

Liu, J., Chen, Z., Elsworth, D., Miao, X., Mao, X., 2010b. Linking gas-sorption induced changes in coal permeability to directional strains through a modulus reduction ratio. International Journal of Coal Geology 83, 21–30.

Liu, J., Elsworth, D., Brady, B.H., 1997. Analytical evaluation of post-excavation hydraulic conductivity field around a tunnel. International Journal of Rock Mechanics and Mining Sciences 34, 181.e181–181.e187.

Liu, J., Wang, J., Chen, Z., Wang, S., Elsworth, D., Jiang, Y., 2011. Impact of transition from local swelling to macro swelling on the evolution of coal permeability. International Journal of Coal Geology 88, 31–40.

Mathews, J.P., Pone, J.D.N., Mitchell, G.D., Halleck, P., 2011. High-resolution X-ray computed tomography observations of the thermal drying of lump-sized sub-bituminous coal. Fuel Processing Technology 92, 58–64.

Mazumder, S., Farajzadeh, F., 2010. An alternative mechanistic model for permeability changes of coalbeds during primary recovery of methane. In: SPE Asia Pacific Oil and Gas Conference and Exhibition. SPE, Brisbane, Queensland.

Menon, V.C., Leon, C.A.L.Y., Kyotani, T., Radovic, L.R., 1991. The effect of moisture on the sorption of gases by coal. Preprint Papers – American Chemical Society, Division of Fuel Chemistry, American Chemical Society, New York, NY, pp. 20-IEC.

Min, K.-B., Rutqvist, J., Elsworth, D., 2009. Chemically and mechanically mediated influences on the transport and mechanical characteristics of rock fractures. International Journal of Rock Mechanics and Mining Sciences 46, 80–89.

Norinaga, K., Kumagai, H., Hayashi, J.-I., Chiba, T., Sasaki, M., 1997. Type of Water Associated with Coal. Argonne National Lab, San Francisco.

Ouyang, Z., Elsworth, D., 1993. Evaluation of groundwater flow into mined panels. International Journal of Rock Mechanics and Mining Sciences and Geomechanics Abstracts 30, 71–79.

Palmer, I., 2009. Permeability changes in coal: analytical modeling. International Journal of Coal Geology 77, 119–126.

Palmer, I., Mansoori, J., 1998. How permeability depends on stress and pore pressure in coalbeds: a new model. In: SPE Annual Technical Conference and Exhibition. Society of Petroleum Engineers, Denver, CO.

Pan, Z., Connell, L.D., 2007. A theoretical model for gas adsorption-induced coal swelling. International Journal of Coal Geology 69, 243–252.

Pan, Z., Connell, L.D., 2012. Modelling permeability for coal reservoirs: a review of analytical models and testing data. International Journal of Coal Geology 92, 1–44.

Pan, Z., Connell, L.D., Camilleri, M., Connelly, L., 2010. Effects of matrix moisture on gas diffusion and flow in coal. Fuel 89, 3207–3217.

Pashin, J.C., 2010. Variable gas saturation in coalbed methane reservoirs of the Black Warrior Basin: implications for exploration and production. International Journal of Coal Geology 82, 135–146.

Pashin, J.C., McIntyre, M.R., 2003. Temperature–pressure conditions in coalbed methane reservoirs of the Black Warrior basin: implications for carbon sequestration and enhanced coalbed methane recovery. International Journal of Coal Geology 54, 167–183.

Pini, R., Ottiger, S., Burlini, L., Storti, G., Mazzotti, M., 2009. Role of adsorption and swelling on the dynamics of gas injection in coal. Journal of Geophysics Research 114, B04203.

Pone, J.D.N., Halleck, P.M., Mathews, J.P., 2010. 3D characterization of coal strains induced by compression, carbon dioxide sorption, and desorption at in situ stress conditions. International Journal of Coal Geology 82, 262–268.

Prinz, D., Littke, R., 2005. Development of the micro- and ultramicroporous structure of coals with rank as deduced from the accessibility to water. Fuel 84, 1645–1652.

Radlinski, A.P., Busbridge, T.L., Gray, E.M., Blach, T.P., Cheng, G., Melnichenko, Y.B., Cookson, D.J., Mastalerz, M., Esterle, J., 2009. Dynamic micromapping of CO_2 sorption in coal. Langmuir 25, 2385–2389.

Reeves, S., 2003. Geologic Sequestration of CO2 in Deep, Unmineable Coalbeds: An Integrated Research and Commercial-scale Field Demonstration Project. Department of Energy, Houstan.

Reucroft, P.J., Patel, H., 1986. Gas-induced swelling in coal. Fuel 65, 816–820.

Robertson, E.P., 2005. Measurement and Modeling of Sorption-induced Strain and Permeability Changes in Coal. Idaho National Laboratory, Idaho.

Robertson, E.P., Christiansen, R.L., 2007. Modeling laboratory permeability in coal using sorption-induced-strain data. SPE Reservoir Evaluation and Engineering 10, 1–11.

Rogers, R.E., 1994. Coalbed Methane: Principles and Practice. PTR Prentice Hall, Englewood Cliffs, NJ.

Schepers, K.C., Oudinot, A.Y., Ripepi, N., 2010. Enhanced gas recovery and CO_2 storage in coalbed-methane reservoirs: optimized injected-gas composition for mature

basins of various coal rank. In: SPE International Conference on CO_2 Capture, Storage and Utilization. New Orleans, LA, USA.

Seidle, J.P., Jeansonne, M.W., Erickson, D.J.,1992. Application of matchstick geometry to stress dependent permeability in coals. In: SPE Rocky Mountain Regional Meeting. SPE, Casper, Wyoming.

Seidle, J.R., Huitt, L.G.,1995. Experimental measurement of coal matrix shrinkage due to gas desorption and implications for cleat permeability increases. In: International Meeting on Petroleum Engineering. Society of Petroleum Engineer.

Shi, J.-Q., Durucan, S., 2005. A model for changes in coalbed permeability during primary and enhanced methane recovery. SPE Reservoir Evaluation and Engineering 8.

Shi, J.-Q., Durucan, S.,2008. Modelling of mixed-gas adsorption and diffusion in coalbed reservoirs. In: SPE Unconventional Reservoirs Conference. Keystone, CO, USA, pp. 291–299.

Siemons, N., Busch, A., 2007. Measurement and interpretation of supercritical CO_2 sorption on various coals. International Journal of Coal Geology 69, 229–242.

Siriwardane, H.J., Gondle, R.K., Smith, D.H., 2009. Shrinkage and swelling of coal induced by desorption and sorption of fluids: Theoretical model and interpretation of a field project. International Journal of Coal Geology 77, 188–202.

Soeder, D.J., 1991. The Effects of Overburden Stress on Coalbed Methane Production, TechBooks, Sponsored by American Association of Petroleum Geologists, Energy Minerals Division, Fairfax, VA.

Somerton, W.H., Söylemezoglu, I.M., Dudley, R.C., 1975. Effect of stress on permeability of coal. International Journal of Rock Mechanics and Mining Sciences and Geomechanics Abstracts 12, 129–145.

Unsworth, J.F., Fowler, C.S., Heard, N.A., Weldon, V.L., McBrierty, V.J., 1988. Moisture in coal. 1. Differentiation between forms of moisture by N.M.R. and microwave attenuation techniques. Fuel 67, 1111–1119.

US-DOE, 2004. Coalbed Methane Premier: New Source of Natural Gas—Environmental Implication, Background and Development in the Rocky Mountain West. National Petroleum Technology Office, p. 77.

van Bergen, F., Krzystolik, P., van Wageningen, N., Pagnier, H., Jura, B., Skiba, J., Winthaegen, P., Kobiela, Z., 2009. Production of gas from coal seams in the Upper Silesian Coal Basin in Poland in the post-injection period of an ECBM pilot site. International Journal of Coal Geology 77, 175–187.

van Bergen, F., Pagnier, H., Krzystolik, P., 2006. Field experiment of enhanced coalbed methane–CO_2 in the upper Silesian basin of Poland. Environmental Geosciences 13, 201–224.

Walker Jr., P.L., Verma, S.K., Rivera-Utrilla, J., Khan, M.R., 1988. A direct measurement of expansion in coals and macerais induced by carbon dioxide and methanol. Fuel 67, 719–726.

Wang, S., Elsworth, D., Liu, J., 2011. Permeability evolution in fractured coal: the roles of fracture geometry and water content. International Journal of Coal Geology 87, 13–25.

Wang, S., Elsworth, D., Liu, J., 2012. A mechanistic model for permeability evolution in fractured sorbing media. Journal of Geophysical Research 117, 1–17, http://dx.doi.org/10.1029/2011JB008855.

White, J.M., Mazurkiewicz, M., 1989. Effect of moisture content on mechanical properties of Nemo coal, Moberly, Missouri, USA. Mining Science and Technology 9, 181–185.

Wolfram Mathematica 7.2, 2009. Uncertainty analysis tool.

Wu, Y., Liu, J., Chen, Z., Elsworth, D., Pone, D., 2010a. A dual poroelastic model for CO_2-enhanced coalbed methane recovery. International Journal of Coal Geology 86, 177–189.

Wu, Y., Liu, J., Elsworth, D., Chen, Z., Connell, L., Pan, Z., 2010b. Dual poroelastic response of a coal seam to CO_2 injection. International Journal of Greenhouse Gas Control 4, 668–678.

Wu, Y., Liu, J., Elsworth, D., Miao, X., Mao, X., 2010c. Development of anisotropic permeability during coalbed methane production. Journal of Natural Gas Science and Engineering 2, 197–210.